OKLAHOMA TRANSPORTATION CENTER

ECONOMIC ENHANCEMENT THROUGH INFRASTRUCTURE STEWARDSHIP

INTERSTATE-35 BRIDGE INSTRUMENTATION RENAISSANCE

J. DAVID BALDWIN, PH.D.
CHRISTOPHER RAMSEYER, PH.D.
THORDUR RUNOLFSSON, PH.D.
ADAM KROLL, M.SC.

OTCREOS9.1-34-F

Oklahoma Transportation Center
2601 Liberty Parkway, Suite 110
Midwest City, Oklahoma 73110

Phone: 405.732.6580
Fax: 405.732.6586
www.oktc.org

DISCLAIMER

The contents of this report reflect the views of the authors, who are responsible for the facts and accuracy of the information presented herein. This document is disseminated under the sponsorship of the Department of Transportation University Transportation Centers Program, in the interest of information exchange. The U.S. Government assumes no liability for the contents or use thereof.

Technical Report Documentation Page

1. REPORT NO.	2. GOVERNMENT ACCESSION NO.	3. RECIPIENTS CATALOG NO.
OTCREOS9.1-34-F		

4. TITLE AND SUBTITLE	5. REPORT DATE
Interstate-35 Bridge Instrumentation Renaissance	September 2012
	6. PERFORMING ORGANIZATION CODE
7. AUTHOR(S)	8. PERFORMING ORGANIZATION REPORT
J. David Baldwin, Christopher Ramseyer, Thordur Runolfsson, Adam Kroll	
9. PERFORMING ORGANIZATION NAME AND ADDRESS	10. WORK UNIT NO.
School of Aerospace & Mechanical Engineering The University of Oklahoma 865 Asp Avenue, Room 212 Norman, Oklahoma 73019	11. CONTRACT OR GRANT NO. DTRT06-G-0016
12. SPONSORING AGENCY NAME AND ADDRESS	13. TYPE OF REPORT AND PERIOD COVERED
Oklahoma Transportation Center (Fiscal) 201 ATRC, Stillwater, OK 74078 (Technical) 2601 Liberty Parkway, Suite 110, Midwest City, OK 73110	Final October 2009- September 2012
	14. SPONSORING AGENCY CODE

15. SUPPLEMENTARY NOTES
University Transportation Center

16. ABSTRACT
An updated, accelerometer-based, sensor and data acquisition system was installed and verified on the I-35 Walnut Creek Bridge in Purcell, Oklahoma. The data collection system also includes a microwave communication system to move sensor and video data off the bridge, through the ODOT proprietary network, to a server on the OU Norman campus. A new approach to structural health monitoring is proposed based on a reliability definition of structural health. Within that framework, the structure's probability of failure is estimated using data from the sensor network, the output of a moving mass analysis to simulate the traverse of a heavy vehicle across the bridge, and a probabilistic metal fatigue analysis incorporating a Markov state transition analysis to map the transition of the structure from the undamaged to failed states.

17. KEY WORDS	18. DISTRIBUTION STATEMENT		
Structural health monitoring, bridge, sensor system, heavy vehicle, moving mass analysis	No restrictions. This publication is available at www.oktc.org and from the NTIS.		
19. SECURITY CLASSIF. (OF THIS REPORT)	20. SECURITY CLASSIF. (OF THIS PAGE)	21. NO. OF PAGES	22. PRICE
Unclassified	Unclassified	38 + covers	

SI (METRIC) CONVERSION FACTORS

Approximate Conversions to SI Units

Symbol	When you know	Multiply by	To Find	Symbol
	LENGTH			
in	inches	25.40	millimeters	mm
ft	feet	0.3048	meters	m
yd	yards	0.9144	meters	m
mi	miles	1.609	kilometers	km
	AREA			
in^2	square inches	645.2	square millimeters	mm
ft^2	square feet	0.0929	square meters	m^2
yd^2	square yards	0.8361	square meters	m^2
ac	acres	0.4047	hectares	ha
mi^2	square miles	2.590	square kilometers	km^2
	VOLUME			
fl oz	fluid ounces	29.57	milliliters	mL
gal	gallons	3.785	liters	L
ft^3	cubic feet	0.0283	cubic meters	m^3
yd^3	cubic yards	0.7645	cubic meters	m^3
	MASS			
oz	ounces	28.35	grams	g
lb	pounds	0.4536	kilograms	kg
T	short tons (2000 lb)	0.907	megagrams	Mg
	TEMPERATURE (exact)			
°F	degrees Fahrenheit	(°F-32)/1.8	degrees Celsius	°C
	FORCE and PRESSURE or STRESS			
lbf	poundforce	4.448	Newtons	N
lbf/in^2	poundforce per square inch	6.895	kilopascals	kPa

Approximate Conversions from SI Units

Symbol	When you know	Multiply by	To Find	Symbol
	LENGTH			
mm	millimeters	0.0394	inches	in
m	meters	3.281	feet	ft
m	meters	1.094	yards	yd
km	kilometers	0.6214	miles	mi
	AREA			
mm^2	square millimeters	0.00155	square inches	in^2
m^2	square meters	10.764	square feet	ft^2
m^2	square meters	1.196	square yards	yd^2
ha	hectares	2.471	acres	ac
km^2	square kilometers	0.3861	square miles	mi^2
	VOLUME			
mL	milliliters	0.0338	fluid ounces	fl oz
L	liters	0.2642	gallons	gal
m^3	cubic meters	35.315	cubic feet	ft^3
m^3	cubic meters	1.308	cubic yards	yd^3
	MASS			
g	grams	0.0353	ounces	oz
kg	kilograms	2.205	pounds	lb
Mg	megagrams	1.1023	short tons (2000 lb)	T
	TEMPERATURE (exact)			
°C	degrees Celsius	9/5+32	degrees Fahrenheit	°F
	FORCE and PRESSURE or STRESS			
N	Newtons	0.2248	poundforce	lbf
kPa	kilopascals	0.1450	poundforce per square inch	lbf/in^2

ACKNOWLEDGEMENTS

We would like to extend our sincere thanks to the following individuals and organizations that helped make this project a reality.

- The Oklahoma Department of Transportation has given us access to the Walnut Creek and Canadian River Bridges for many years as resources to conduct our research. Having access to these structures is vitally important to our investigations, past, present, and future.
- The City of Purcell, Oklahoma provides A/C power to the Walnut Creek Bridge.
- Mr. Alan Stevenson and Mr. Dwayne Cranford of the ODOT Network group provided invaluable aid in specifying and installing the microwave data communications link at Walnut Creek.
- The efforts and assistance of Dr. Joseph Havlicek and Mr. Ekasit Vorakitolan of the University of Oklahoma Intelligent Transportation Systems Laboratory were essential in establishing the data link.
- Dr. Victor DeBrunner and Dr. Linda DeBrunner, Florida A&M University, were involved in the prior related project and were the source of many ideas realized in this project.
- Dr. Kim Mish, Sandia National Laboratory, created the original vision and framework for the project.

INTERSTATE-35 BRIDGE INSTRUMENTAION RENAISSANCE

Final Report

September 30, 2012

J. David Baldwin, Ph.D.
Associate Professor, Principal Investigator

Christopher Ramseyer, Ph.D.
Assistant Professor, Co-Principal Investigator

Thordur Runolfsson, Ph.D.
Professor, Co-Principal Investigator

Adam Kroll, M.Sc.
Graduate Research Assistant

Sponsoring Agency
Oklahoma Transportation Center
2601 Liberty Parkway, Suite 110
Midwest City, Oklahoma 73110

TABLE OF CONTENTS

LIST OF FIGURES

EXECUTIVE SUMMARY

The primary aims of this project were to install a new sensor system with data acquisition on the I-35 Walnut Creek Bridge (WCB) in Purcell, OK, and to continue the development of algorithms that will implement structural health monitoring on that bridge. A sensor system consisting of 12 accelerometers was installed on two of the four spans of the WCB with a computer-based data acquisition system controlling the data collection and storage. The operation of the data acq system demonstrated the capability of collecting data during the passage of one or more heavy vehicles, while going into a passive mode during the passage of light vehicles, e.g., passenger cars, or when no vehicles were present on the bridge. A microwave-based data transmission system was activated at the bridge to transmit accelerometer data and a video stream from the bridge to a server on the University of Oklahoma Norman campus.

In addition to the implementation of the data acquisition hardware, our efforts were focused on the analyses required to conduct a health assessment on the bridge based on probabilistic measures. We have proposed a working definition of the "health" of a bridge as being its probability of survival, i.e., its *reliability*. This is in contrast to others who use structural responses as the measure of health, without defining the measure of health itself. In order to translate the global scale bridge responses such as accelerations to local scale responses such as stress and strain, we further propose that the moving mass analysis (simulating the passage of a heavy vehicle across the bridge) provides the necessary link. This report outlines several finite-element based computer simulations of simple moving load/mass problems and demonstrates very good agreement with analytical solutions. Further, we have explored three-dimensional FE simulations that have no analytical solutions available. The local stress/strain results of these simulations will feed directly into the structural health assessment estimates.

1.0 INTRODUCTION

For well over a decade, engineers at the University of Oklahoma have studied bridges south of the Norman campus on Interstate 35. This research enterprise began with the pioneering work of the late Professor William Patten [1], who deployed sensors and semi-active control devices to damp bridge oscillations on an I-35 overpass over Walnut Creek. Over this period, sensor and communication technologies have seen spectacular improvements in cost, reliability, and performance, and with these technological improvements we set out to conduct new research that can lead to gains in our ability to estimate both the loads that are applied to these bridges, and also the damage done to them by those vehicle loads. The first goal of this was project was to upgrade the sensors and network systems on the Walnut Creek Bridge (WCB) so that research can advance on the all-important front of insuring the safety of national shared infrastructure.

In addition to the new sensor system, our work included applied research efforts to prove the concept that the vibrations of these bridges can be evaluated using stochastic estimation methods coupled with advanced finite element models for structural response, to gain both accurate estimates of vehicle loads over time, and good estimates of structural reliability for these bridges. Both of these estimates are of considerable value to practicing bridge engineers at the Oklahoma DOT in their quest to provide safe and reliable transportation systems, and the estimation methods are of great research value to the nation.

Many studies have been done concerning the use of accelerometer sensor systems on large interstate highway bridges, including Bhachu [2] and Patten [2]. These systems were used to gather information ranging from the material and system properties of the bridge, to identification of vehicles and weight approximations. Using accelerometers as the primary sensors provides benefits over other transducer types for the purpose of this project, by providing structural response information on a large, or *global*, scale. As the end goal of the analysis portion of the project was the statistical approximation of life through damage accumulation, *local* stress-strain histories must be created for the vehicle-bridge interactions. Local sensors such as strain gauges would directly deliver this at select locations, but would provide an incomplete view of the overall bridge response. We propose that acceleration data can provide the requisite data for input to the fatigue-based structural degradation model, through the incorporation of results from solutions to the moving mass problem on beams and plates, thus providing estimated deformation and strain profiles for the bridge. An unknown model uncertainty would be introduced to the analysis by the moving mass analysis, but we feel that the uncertainty can be quantified and managed.

Accelerometers are robust instruments compared to strain gauges. Accelerometers are often designed to withstand large impacts, extreme temperature changes, and even high humidity, whereas strain gauges are typically composed of a circuit with a few wires, whose only protection is the adhesive used to attach it to the surface. To that point, strain gauges are attached through the use of adhesives, while accelerometers can be stud mounted, adhered, or attached with a magnetic base. Although the noise level increases as you progress from the former to the latter, the bridge in this study is not allowed to be modified or affixed with permanent measures, and thus only the magnetic option remains. While more expensive in their first cost, we used accelerometers in this project because of their global response characteristics, robust construction, and ease of installation, compared to strain gages or direct

displacement measurement devices such as linear variable differential transformers (LVDT's) or string potentiometers.

In addition to work on specifying, installing and validating the new WCB sensor system, we have focused on the use of the structural response data coming off the bridge. Specifically, we were interested in making a connection between the global response, as captured by the accelerometers, and the local response (i.e., on the length scale of centimeters) where the damage processes occur that lead to structural failure. The impetus for making this connection was the development of structural health monitoring (SHM) paradigm based on probability of structural survival (or *reliability*) being the measure of health. Many prior studies have purported to conduct SHM, but none have proposed quantifiable measure for health. Using this framework, we have identified the moving mass problem, most frequently applied to simple beam systems, as the link between the global and local behavior of the bridge structure. In the sections that follow, these two essential elements to a rational SHM methodology are outlined.

2.0 THE BRIDGE SENSOR SYSTEM

The Walnut Creek Bridge (WCB) consists of two 2-lane, 4-span, 45º skew bridges (north- and south-bound) on Interstate I-35 in Purcell, Oklahoma consisting of a 7.5 inch (0.19 m) thick deck above five continuous W54X142 girders. Transverse diaphragms appear perpendicular to the beam length approximately every 20 feet (6.096 m). A top view and section view of the north-bound bridge are shown in Figure 1 [1].

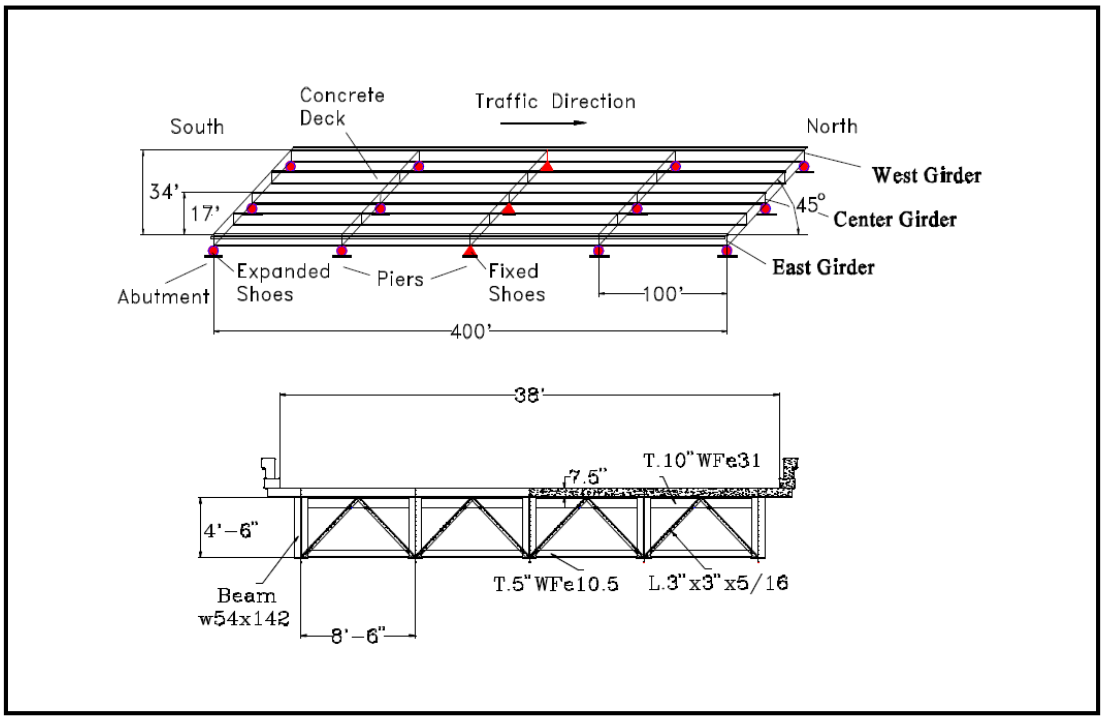

Figure 1: Top and Section Views of North-Bound Walnut Creek Bridge

Figure 2 shows how the traffic lanes are oriented with respect to the bridge's girders. In the Figure, the girders are shown by solid lines, and the traffic lane boundaries are shown as dashed lines. Note that there is a wide shoulder to the right of the right lane.

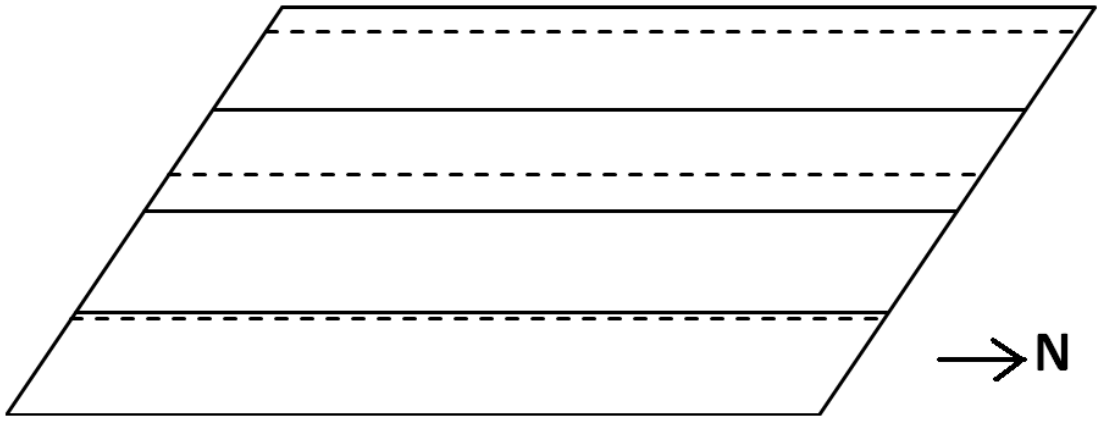

Figure 2: WCB Traffic Lane Orientation Relative to Girder Position

The Walnut Creek Bridge is often an inhospitable environment for electronic devices. Temperatures underneath the bridge deck can vary from below freezing to well over 100ºF over the course of the year. Additionally, the creek below the bridge has been known to flood to the extent of submerging the lower sections of the bridge. Animals often take shelter in the bridge, and expensive devices are often stolen from public locations. As such, it is necessary for the sensor system to be robust, water resistant, discreet, and secure.

The instrumentation systems selected for the bridges consist of a central data acquisition computer, power supply elements, accelerometers, signal conditioners, cabling components, data acquisition software, and basic data analysis software. The components we selected were chosen on the basis of their commercial availability, ability to withstand long term exposure to the elements when installed on the bridge, and their efficient power demands when appropriately configured.

2.1 Data Acquisition Subsystem

The central component in the instrumentation chain is the data acquisition computer. We chose the SoMat eDAQlite, Figure 3, for its known outstanding performance in difficult environments. It has a robust water-resistant aluminum casing that will provide protection against humidity, can support sample rates in the desired region, has an operating range covering expected temperatures, has a large flash memory for storing data between retrievals, and is able to transfer data quickly through an Ethernet connection. Our system is configured for 16 channels of differential analog data (with the possibility of adding more if conditions dictate) with 32 GB of on-board memory. Currently our system is set up for DC operation from an integral battery pack; we could re-configure to AC as necessary.

Figure 3: SoMat eDAQlite Data Acquisition System [3]

2.2 Accelerometers

Based on prior studies on the Walnut Creek Bridge, we expect maximum accelerations to be between 1 and 5 g. Also, based on prior data, the first ten resonant frequencies of the bridge have been observed at less than 20 Hz. We chose the PCB model 393A03 ICP accelerometer, Figure 4, for our sensor as it has an acceleration range of ± 5 g at 0.5-2,000 Hz.

Figure 4: PCB Model 393A03 Accelerometer [4]

2.3 Signal Conditioning and Cabling

To provide accelerometer signal condition, we use SoMat EICP-B signal conditioning modules suitable for accelerometer sensors. The EICP-B units are connected to the eDAQ by SoMat 1-SAC-TRAN-2-2 cables that provide the proper jacks for interfacing with the eDAQ plugs. We used RG-59 22 AWG coaxial cable with MIL-C-5015 2-pin connectors to make the connections between the accelerometers and the signal conditioners. The accelerometers are attached to the top of the girder bottom flanges using PCB 080A121 magnetic bases.

2.4 Sensor System Installation and Checkout

Figure 5 shows the accelerometer installation schematic for the Walnut Creek Bridge. This figure only shows the two north-most spans of the four-span bridge. There are five girders running the length of the two-lane bridge, and the accelerometers are placed along the interior girders. The western-most girder corresponds to the left lane boundary parapet, the middle girder to the center of the right lane, and the eastern-most girder to the shoulder parapet. In the fourth span, the sensors were installed at the half and third points of the span, i.e., ~33 ft. (10.1 m), 50 ft. (15.2 m), and 67 ft. (20.4 m) from the North abutment; this arrangement of sensors precludes simultaneous coincidence with the nodes of bending vibration until the sixth bending mode. In the third span, the sensors were installed at mid-span, i.e., ~50 ft. (15.2 m) south of the pier. The data acquisition computer is located in the third span, where a decking system is installed to support workers, equipment, etc.

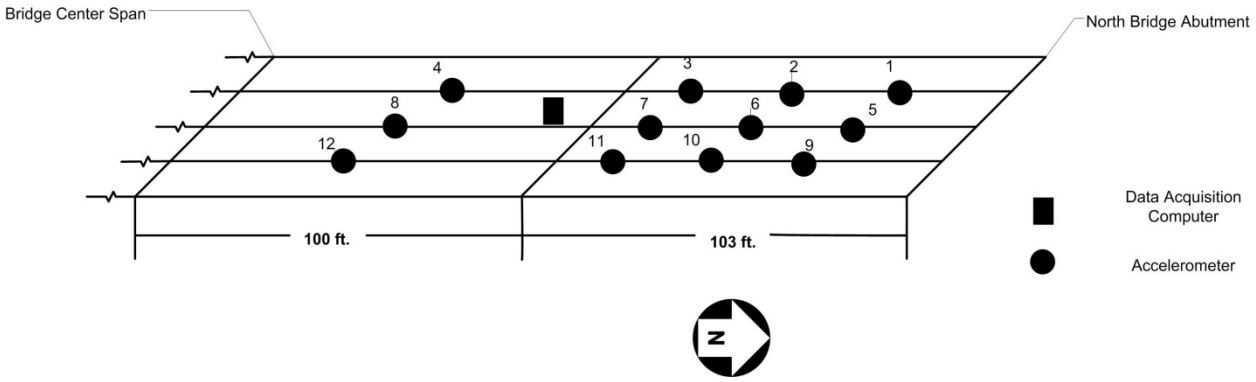

Figure 5: Walnut Creek Bridge Sensor Installation Map (Plan View)

With the sensor system installed, we set out to verify its function and to begin the process of characterizing the traffic flowing over the bridge. In what follows, we outline the initial process used to observe the response of the bridge structure to live traffic using our sensors, from short-term data collection and the capture of vehicle characteristics (e.g., vehicle type and lane), to the development of a software tool to assist in the assessment of the bridge response in the frequency domain to five different representative heavy truck types in single and multiple formation.

As part of our system setup and qualification, we recorded approximately 30 minutes of continuous data from the nine installed and operational sensors in the grid; the data was recorded from approximately 11:50 a.m. to 12:20 p.m. on a Friday morning in December 2011. As an example of the data, Figure 6 shows the time histories from channels 5-7 from the north span's central support girder (i.e., approximately the bridge right lane centerline). From the Figure we see that the maximum/minimum accelerations are in the range of ± 0.15 g's and that there appear to be clear delineations between acceleration events. The other recorded channels showed similar characteristics. As will be discussed below, these data were generated by the passage of a variety of vehicles traveling north-bound on I-35 and should be representative of the bridge response over time.

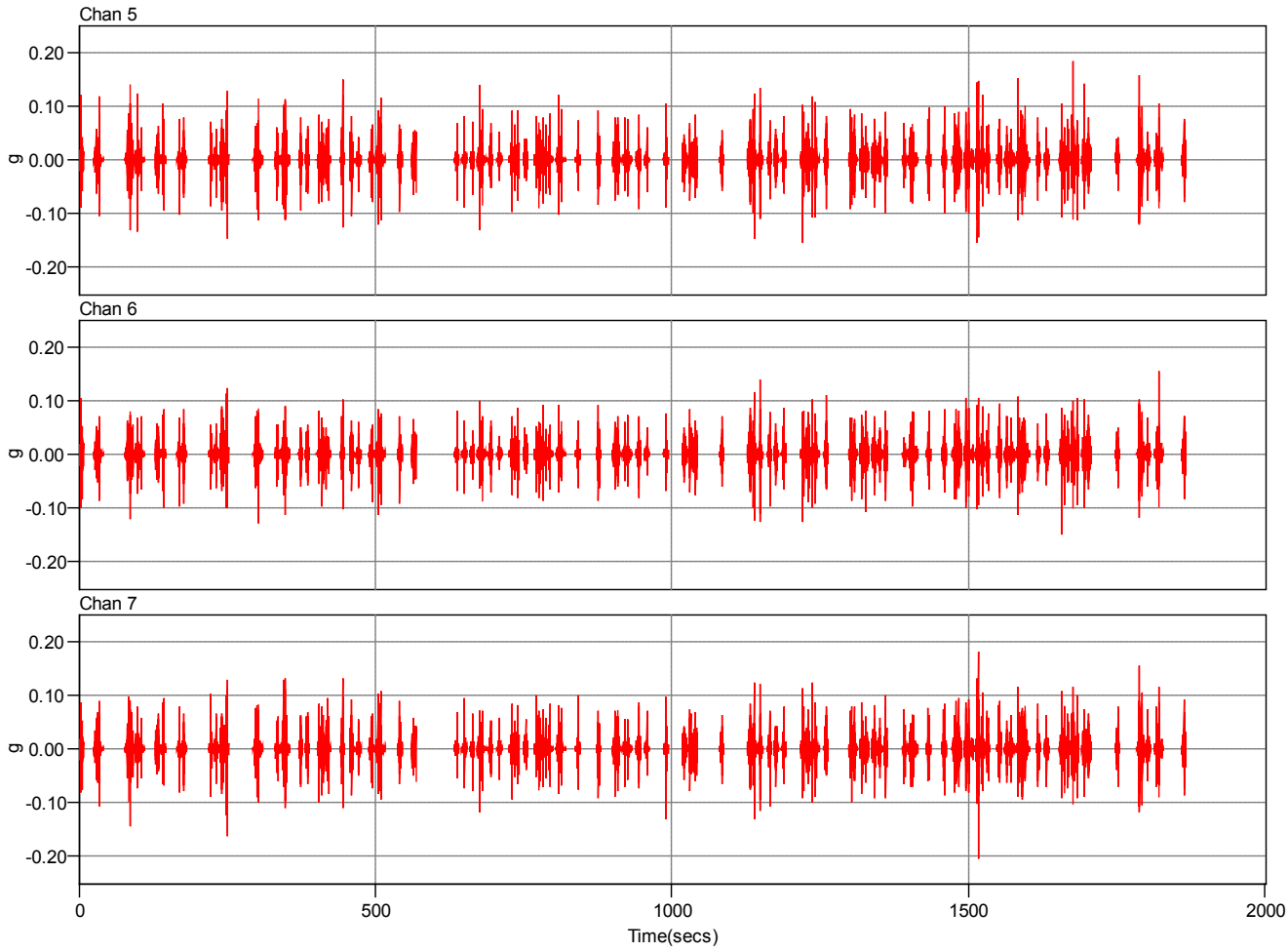

Figure 6: Thirty-Minute Acceleration Time Histories from Channels 5-7

During the test time represented in Figure 6, a voice record was made describing the passing vehicles and their approximate time stamps within the test. The voice record transcription for this test record is included below, with the time (in square brackets) representing the elapsed time after the start of data recording; the designation Right/Left indicates the traffic lane the vehicle occupied, ellipsis ("…") indicates a short passage of time, and the vehicle description is an attempt to characterize the passing vehicle.

[00:05] (N/A) Semi {double}
[00:38] (Left) Semi (Right) Semi (Right) Semi
[01:20] (Right) Tank (Right) Rock (Right) Semi ... (Right) Flatbed {pipe} ... (Right) Semi
[02:04] (Right) Van (Left) Semi ... (Right) Semi
[02:48] (Right) Flatbed (Right) Tractor {cabs}
[03:40] (Right) Semi ... (Right) Van ... (Right) Semi (Left) Grain ... (Left) Semi (L&R) Flatbed {crane} & Semi
[04:55] (Left) Rock (Right) Rock
[05:33] (Right) Bus (Right) Flatbed {empty} ... (Right) Flatbed {empty} (Right) Semi {double}
[06:14] (Right) Semi ... (Right) Semi
[06:45] (Right) Semi ... (Right) Flatbed {empty} ... (Left) Grain
[07:25] (Right) Tractor {cabs} ... (Right) Truck (Right) Pickup (Right) Tractor ... (Left) Semi
[08:10] (Right) Semi (Right) Semi

[08:22] (Right) Semi {short} ... (Right) Rock
[09:00] (Right) Flatbed {equipment}
[09:21] (Right) Cattle {empty} (Left) Rock (Right) Semi
[10:37] (Right) Semi
[10:50] (Right) Semi
[11:04] (Right) Semi
[11:15] (Right) Semi (L&R) Rock & Semi
[11:33] (Right) Semi
[11:50] (Right) Pickup
[12:08] (Right) Flatbed {equipment} (Left) Pickup (Right) Semi (Right) Semi
[12:30] (Right) Pickup (Left) Flatbed {empty}
[12:50] (Right) Tank (Right) Semi (Right) Tank (Right) Tractor (Right) Tractor ... (Right) Semi
[13:27] (Right) Tank ... (Right) Semi
[14:00] (Right) Tractor {automobiles}
[14:35] (Right) Semi
[15:03] (Right) Semi ... (Right) Semi
[15:19] (Right) Semi ... (Right) Grain
[15:44] (Right) Rock
[15:57] (Right) Truck
[16:29] (Right) Flatbed {pipe} (Right) Truck ... (Left) Tractor
[16:59] (Right) Semi
[17:10] (Right) Flatbed {empty} ... (Left) Semi (Right) Semi
[18:03] (Left) Semi
[18:51] (Right) Semi (Right) Rock
[19:08] (Right) Flatbed {pipe}
[19:23] (R&L) Semi & Semi
[19:34] (Right) Semi
[19:48] (Left) Rock
[20:12] (Left) Truck
[20:20] (Right) Flatbed {pipe} (Left) Semi (Left) Rock (Left) Rock ... (Right) Tractor {cabs} (Right) Tractor {cabs}
[20:59] (Right) Semi
[21:23] (Left) Tank (Right) Flatbed {empty}
[21:40] (Right) Tank ... (Left) Tractor {cabs}
[21:59] (Right) Semi ... (Right) Semi ... (Left) Truck ... (Right) Semi ... (Right) Truck (Left) Grain
[22:38] (Left) Flatbed {truck} (Right) Semi
[23:13] (Right) Truck
[23:20] (Right) Tank (R&L) Semi & Rock
[23:51] (R&L) Truck & Flatbed
[24:19] (Right) Semi {double}
[24:36] (Right) Flatbed {pipe} (Right) Semi (Right) Tank
[24:55] (Right) Cement (Right) Flatbed {loaded}
[25:15] (Right) Flatbed {loaded} ... (Right) Semi {double}
[25:30] (Right) Semi
[25:50] (Right) Rock
[26:03] (Left) Grain ... (Right) Tank
[26:23] (Right) Tractor {cabs} ... (Right) Semi ... (Right) Semi {short} ... (Right) Semi
[26:57] (Right) Pickup {trailer}
[27:10] (Left) Semi {double}
[27:35] (Right)Rock (Left)Semi ... (R&L) Semi & Semi ... (Right)Semi ... (Right)Rock ... (Right)Flatbed{empty}

[28:13] (Right) Rock ... (Left) Rock
[28:54] (Left) Grain
[29:10] (Left) Grain
{29:46] (Right) Semi {double} (Left) Flatbed {car} (Right) Truck ... (Right) Semi
[30:17] (Right) Pickup (Right) Right

In order to improve and automate our data analysis of the acceleration time histories coming off our bridge data acquisition system, e.g., Figure 6, we built a MATLAB program to read the acceleromter data histories and provide basic data cleansing and qualification operations. It is essential that we be able to read the incoming data sets, check the data for anomalies such as missing sensor signals, classify the passing vehicles and estimate their weight, speed, and lane, and curate the data to assure it is named and stored properly. To facilitate the anticipated structural health monitoring (SHM) analyses and to automate them to the maximum extent possible, our MATLAB program, Figure 7, has been developed. This program bundles several analysis functions into a single interface and magnifies our ability to conduct analysis in time.

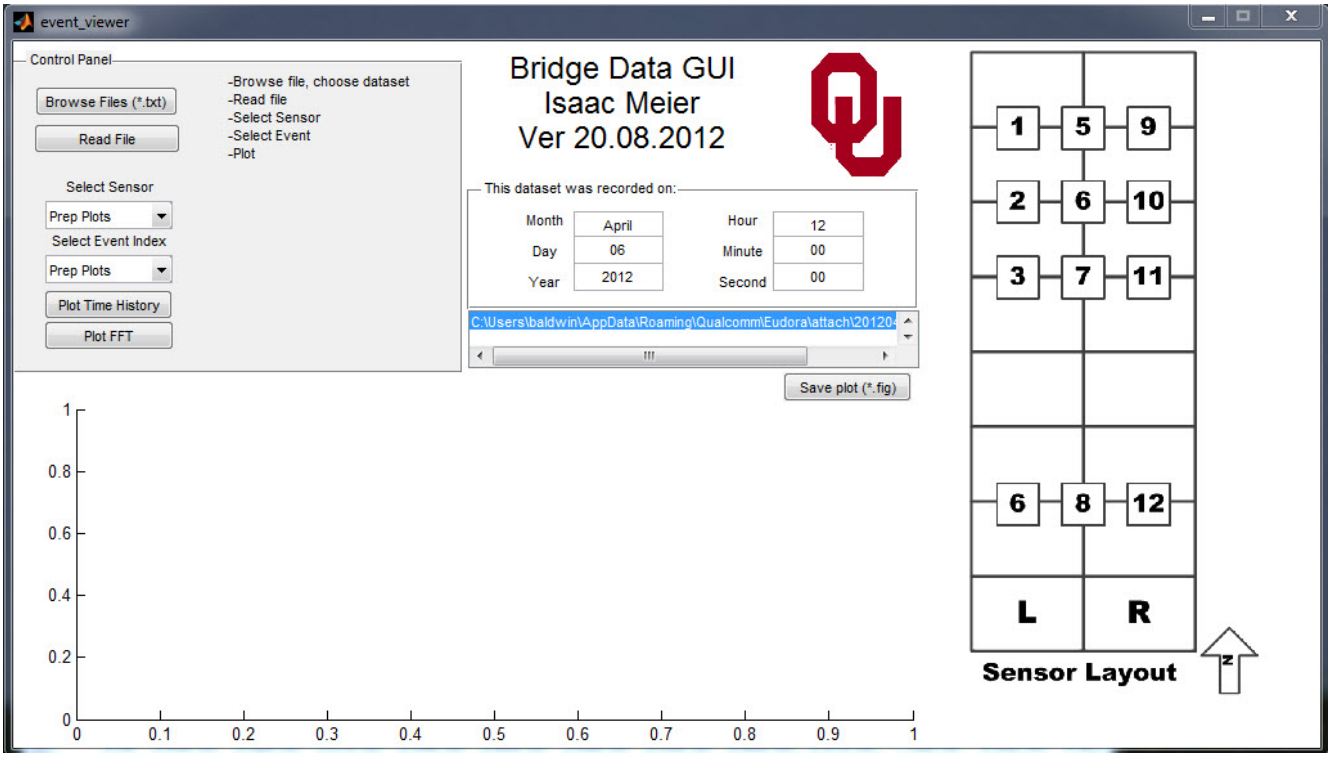

Figure 7: MATLAB event_viewer Program Interface

We have used this software tool to closely examine, in the frequency domain, our acceleration data correlated with the passing vehicle type. In the process, we observed the complications involved in discerning vehicle type from the acceleration time histories. As an example, Figure 8 shows the frequency response of the bridge to the passage of one, two, and four sequential tractor trailer vehicles in the right lane. In the case of the multiple vehicles, they were traveling close enough together to suggest that they might be considered as a single vehicle. The Figure shows, however, that the single vehicle dominates the lowest frequency peak, while the quad and double vehicle sets dominate the second/third and fourth/fifth peaks, respectively. Given the commonplace nature of such vehicle passages, these results highlight the importance of further developing analysis methods that are robust to multiple vehicle types and spacings.

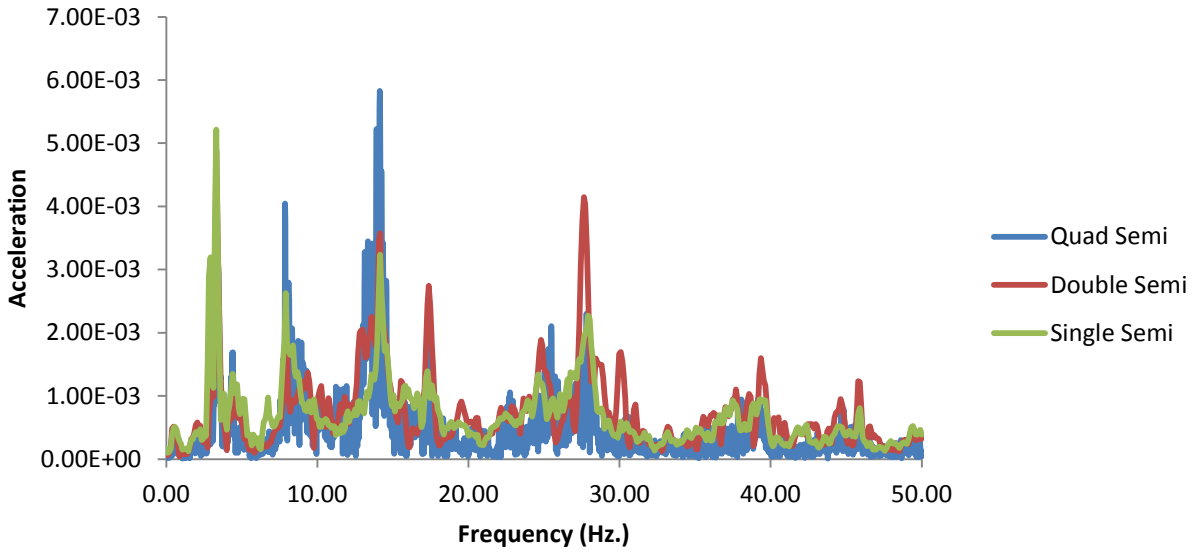

Figure 8: Frequency Domain Comparison of Multiple Vehicle Passages

As a further illustration of the differences we have observed in the bridge response to the passage of different vehicle types, Figure 9 gives a comparison between a single tractor-trailer, a single tanker truck, and a single (empty) flatbed truck. Again, we see that the frequencies show consistencies, e.g., ~3 Hz., but we also see that between 5 and 10 Hz., the different vehicles seem to be exciting the bridge at inconsistent frequencies. It is possible that the potentially widely varying weights of these three vehicle types, combined with their different suspension characteristics, do in fact excite the bridge differently; more data and analysis will illuminate this phenomenon, however.

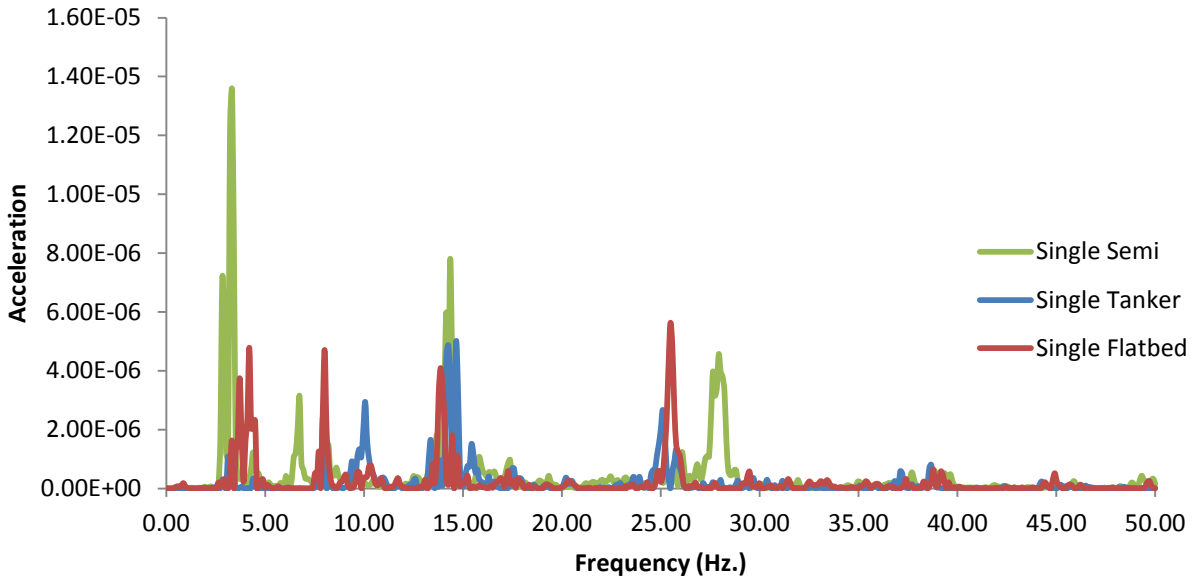

Figure 9: Frequency Response: Three Vehicle Types

Our rationale for focusing on the dynamic response of the bridge as illustrated above is based on the continued development of our structural health monitoring paradigm for bridges, Section 3 below. In order to assess the health of a structure such as a bridge, the analysis must span length scales from the global (length scales in feet), where we observe the overall motion of the structure, to the local (length scales in inches), where damage mechanisms occur that lead to structural failure. Our working model for this analysis uses the moving load problem from mechanics to connect the two length scales. As we continue to develop this model, we will need the sensor outputs from our bridge, along with calibrating vehicle passes (i.e., known weight, speed, suspension geometry, etc.) to permit on-line vehicle identification.

2.5 Microwave Data Transmission Link

The final piece of the refurbished Walnut Creek Bridge is a microwave data communication system. A set of Motorola Model 5700 transmitter/receivers, along with an Axis Model 233D PTZ camera, are installed to provide a video/data link from the bridge to a port on the Oklahoma Department of Transportation network, and from there to a port on the University of Oklahoma network. Figure 10 below shows the schematic of the data connection. The bridge node is at the bottom of the figure. There A/C power is provided by the City of Purcell to operate the microwave transmitter and the camera. Approximately 2.6 miles (4.2 km) north of the bridge, a receiver/transmitter pair is mounted on a telephone pole; these devices receive power from a bank of batteries charged by a solar panel mounted on the pole. From this position the signal is sent approximately 1 mile (1.6 km) to the northwest where it is received by a receiver mounted on a pole outside the ODOT residence office. This receiver is powered by A/C power provided by ODOT. The data moves onto the ODOT secure network at this location. At the University's Intelligent Transportation Systems laboratory (on the North Campus research zone), the data is moved from the ODOT proprietary network to the University's internal network and then to a data server.

Figure 10: Schematic of the Microwave Communications Link at Walnut Creek

3.0 A PROPOSED NEW PARADIGM FOR STRUCTURAL HEALTH MONITORING

The very active research field of Structural Health Monitoring (SHM) has as its primary goals 1) making an estimate of the current load carrying capacity (static strength) of a structure, and 2) making an estimate of the remaining life of the structure under its operating conditions. The majority of papers published recently on SHM seem, rather, to be focused on the instrumentation and qualitative analysis of the dynamic responses. These efforts could properly be labeled Structural Response Monitoring (SRM) instead of SHM. Lacking the element of residual strength and/or life analysis, they do not represent SHM, per se. It is proposed that, to implement SHM in its entirety, a critical link be created between the global, dynamics-based response given by the monitoring systems and the local structural damage models that are used in structural integrity analyses. This link, for bridges, we propose would be based on the vehicle/structure interaction models available for moving loads/masses.

As noted by McCabe, the way forward in assuring bridge performance is based on a probabilistic framework (emphasis added):

> "The way to ensure the safety of our nation's aging bridge infrastructure is: first, a consistent and rational, **risk-based bridge-inspection program**; second, a dedicated funding methodology for structurally deficient bridges; and third, use of advanced technologies and materials. The probability of a bridge failure is extremely low; however it is not zero. Let's not wait for the next failure." [5]

This focus on using the probabilistic notion of risk is further emphasized by an Oregon group stating

> "Shifting to a risk-based bridge inspection program that would allow states to define a risk-based inspection frequency and level of inspection based on the level of vulnerability to damage rather than requiring that all bridges be inspected every two years, regardless of structural problems or risk;" [6]

These two statements suggest that there is a desire in the bridge engineering community for risk-based methods of bridge structural integrity analysis as it applies to the structural health assessment of structures. The concept of risk is often used casually to refer to some potentially hazardous condition. In engineering analysis, risk typically takes on a more specific meaning that combines the probability of occurrence of an event with the consequences of the event. One of the commonly used definitions for the risk of an event is [7]

$$Risk = (Event\ Probability\ of\ Occurrence) \times (Cost\ of\ Occurrence) \qquad (1)$$

where the risk can be express in monetary terms. Based on this definition, a high probability-high cost event will carry more risk than a high probability-low cost event.

3.1 Definition of "Health"

One of the key elements in a structural health assessment is a clear, quantitative definition of "health". Currently, there is no consensus in the research community on this definition, although other techniques in the area of structural integrity can be consulted for guidance. The goal here is to establish a working definition of structural health that is consistent with the probabilistic definition of risk above.

We propose that, analogous to the concept of cumulative damage in metal fatigue analysis, we consider the characteristic "unhealth" to be the quantifiable measure, rather than health. To see this distinction, consider a brand new, pristine, undamaged structure as it enters service for the first time. In the simplest scenario, we would say that this structure's "health" is 100% and it's "unhealth" is 0%. As the structure endures service loading, it is exposed to time varying (dynamic) loads, thermal cycling, chemical attack (e.g., ice melting chemicals applied in the winter), and other effects. The result of these "loads" is to cause deterioration of the structure, either by means of metal fatigue, concrete fatigue, chemical attack or others. Most damage mechanisms are accounted for by attempting to quantify the accumulation of damage within the structure, i.e., its progress toward its ultimate state of "unhealth".

As the service loading continues, and damage accumulates, the quantitative measure of "unhealth" increases until it reaches some limit value corresponding to an "unhealth" value of 100%, or complete structural failure. The definition of 100% unhealth varies among the structural damage models. For instance, stress-based fatigue analysis has its limit state defined as complete fracture of a structural element. When using a strain-based fatigue analysis, however, the limit state is the appearance of a small (~10 mm) crack in the element. A fracture mechanics analysis, like the stress-based approach, also has a fracture limit state, but only after consideration of the propagation of the critical crack to a critical length. Clearly the limit state implicit in a given damage model is central to that model's predictive capability.

Based on these considerations, it seems appropriate to then define structural "health" in terms of its "unhealth", a quantity that is tracked by damage models. Some possible ways of relating these quantities are

$$health = 1.0 - unhealth \tag{2}$$

$$health = {}^{1.0}/_{unhealth} \tag{3}$$

Clearly, a number of other equation forms are candidate representations. For purposes of this work, Equation 2 will be the preferred form for the definition of structural health.

3.2 Reliability Analysis

Stated simply, the reliability, $R(t)$, of a structure is defined as the probability of survival, $\Pr(S)$. In this context, survival means that the structure is still capable of carrying its service loads at the given time, t. Conversely, the probability of failure, $F(t)$, is the probability that the structure can no longer carry its loads and has ceased to be in service. Probability theory tells us that for these two mutually exclusive events, the relationship between reliability and failure is

$$R(t) = 1.0 - F(t) \tag{4}$$

From this expression, we can see that there is the beginning of a link between structural "health" and structural reliability. If we think of "health" as the continued ability of the structure to carry its service loads, and "unhealth" as the failure of the structure, these concepts merge and a structural reliability framework emerges as the natural way to discuss structural health. In this context then, $F(t)$ becomes the probability of reaching the limit state of the damage model at the current time.

The question arises at this point, "Why bother with a reliability analysis, when there are so many unknowns involved in the analysis?" When conducting a reliability analysis of any structural element, either statically or dynamically loaded, we have to quantify the probability structure of the loading terms and of the response terms. In the case of a simple statically-loaded element, the probability of failure can be expressed as

$$Pr(Failure) = Pr(stress > strength) \tag{5}$$

The stress term involves uncertainties (ideally expressed as probability density functions, or pdf's) in external loads, structure geometry and constitutive properties. These are combined into a master pdf for stress. Similarly, the strength term takes account of the probability structure, i.e., a pdf, of the relevant strength (yield, ultimate), which comes from replicated laboratory tests. Clearly, even in this simplest case, there is a great deal of probabilistic information that is required to make the $F(t)$ estimate. In principle, the easiest pieces of information are the pdf's for strength and geometry, because they can be measured under controlled circumstances. The load pdf, however, is much more difficult to estimate because we typically measure structural response such as acceleration (by accelerometers) or strain (by strain gages) and these have to be translated into force. Replicating all of the operating conditions the structure might experience becomes difficult if not prohibitive.

The $F(t)$ estimate in a dynamic load environment is even more complicated. The tests required to establish pdf's for the strength measure are typically life tests of one type or another, and can take many hours to complete for a single specimen. Thus replicated strength data is difficult to acquire inexpensively, but in principle it can be done. Similarly, now that the loads are dynamic, there is even more uncertainty in the load pdf, especially if the loading process is nonstationary in time. The instrumentation requirements usually have stopped investigators from collecting enough data to estimate the load pdf's with any clarity.

A new situation presents itself. As we install structural response monitoring systems on bridges and begin to collect data, we might be able to estimate the loading pdf's for a specific structure and get past the factor that has been the most prohibitive in implementing structural reliability analysis in its fullest realization. If we can agree that reliability theory is the correct language for discussing structural health monitoring (true "health" monitoring, not just SRM), then we have a beginning point for this pursuit. By casting the SHM problem in terms of reliability, we also have the framework to incorporate uncertainty analysis involving the instrumentation and data acquisition package used to capture the data.

3.3 Markov Chain Analysis of Structural System Reliability

We will treat a given structure as a system composed of multiple individual elements, each capable of sustaining progressive damage from the loading imposed on the structure. As the structure ages, it will receive ambient loading that induces stresses and strains that are of sufficient magnitude to activate damage processes on a microstructural level within the structural components. Because the individual structural components will experience damage at different levels and rates, we must consider the ultimate failure of any of the components at a given time.

We will use a system reliability model based on the theory of Markov processes to estimate the overall reliability (and thus health) of the structure. The essential first step in this analysis [7] is the establishment of a list of "states" the system can be in during its lifetime. The states of the

system are related to its condition and will take the form of statements such as “State 0 indicates that the structure is in its pristine, as-new condition, with no discernible damage”, “State N indicates that structural element X has experienced sufficient damage to be considered failed”, and so on. The structural details of each system will dictate the states, but defining the system states will be a non-trivial exercise. The resulting Markov model will contain state transition probabilities that express the evolution of the system from its initial undamaged state, through a number of intermediate states defining the progressive damage in the system, to the ultimate, failed state where the structure is no longer able to carry its mandated loads. We will use the probability of being in this failed state, i.e., $F(t)$, to estimate the structural probability of survival, the reliability, the “health” of the structure.

A Markov process is a type of random process that has as its key assumption that the probability of any state transitions at the current time is dependent only upon the current condition of the system, not on any of its past states or conditions [8]. In this sense, the Markov process is considered to be “memory-less” in that future state transitions do not depend on how the system reached its current state, only that it is in that current state. Three other assumptions will be imposed on the Markov process to be used here:

1. The number of system states will be finite and countable. This condition will render our process a “Markov chain”.
2. Time will evolve in a discrete manner, with specified time increments, Δt.
3. It is typical in Markov chain system analysis to assume that the state transition probabilities are constant throughout the analysis. We will relax this assumption of process stationarity and permit them to take on different values that represent the accumulation of damage in the system.

To illustrate this analysis framework, Figure 11 shows a simple two-state Markov chain where State 0 represents an operational system, and State 1 a failed system. The parameter λ represents the instantaneous failure transition probability which controls the transition from operational to failed states. The possibility of repair is expressed by the parameter μ.

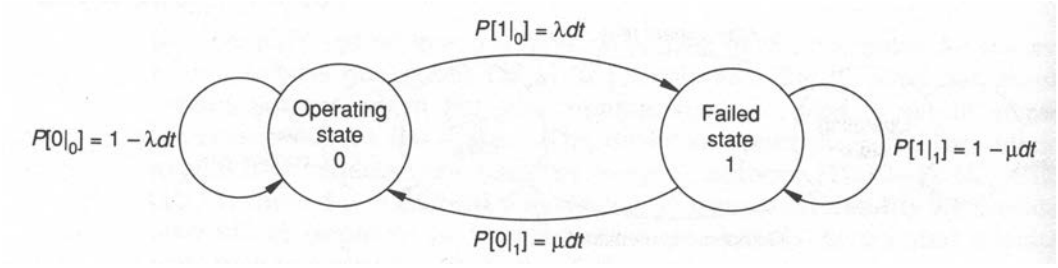

Figure 11: Two-State Markov Chain [8]

Thus we propose constructing a nonstationary, discrete time Markov chain model of the structural system with the goal of estimating its probability of survival, or reliability, as the quantitative measure of the structure’s health [9-12]. The central quantity required to implement the Markov chain model are the state transition probabilities λ and μ; those will have to be determined based on more detailed analysis of the material failure behavior in the structure.

3.4 Information Flow in SHM

In order to conduct a proper structural health assessment, we must work with recorded responses (static and dynamic) observed in the structure. Figure 12 summarizes the interplay of the dynamic loads acting on the structure (heavy trucks in this instance), data recorded from

the global response of the dynamic structure (e.g., accelerometer time histories), and the estimation of the local response of the structural elements (e.g., stresses, strains, etc.) that are essential to the structure's health estimation outlined above. We propose that a detailed analysis of the dynamic response of the bridge caused by the moving vehicle is the essential link between the global and local responses. Because these analyses are typically based on the mechanics of beams and plates, their results are easily stated in terms of the various stresses that occur in those common structural elements. For other structural systems, the link between the global scale responses and the local scale responses will involve other analytical tools, we believe that the moving vehicle models offer the best approach for crossing the analysis gap shown in Figure 12 for bridges. There are a variety of analytical and computational results available in the field of moving load/mass analysis and several of those will be discussed in the next section.

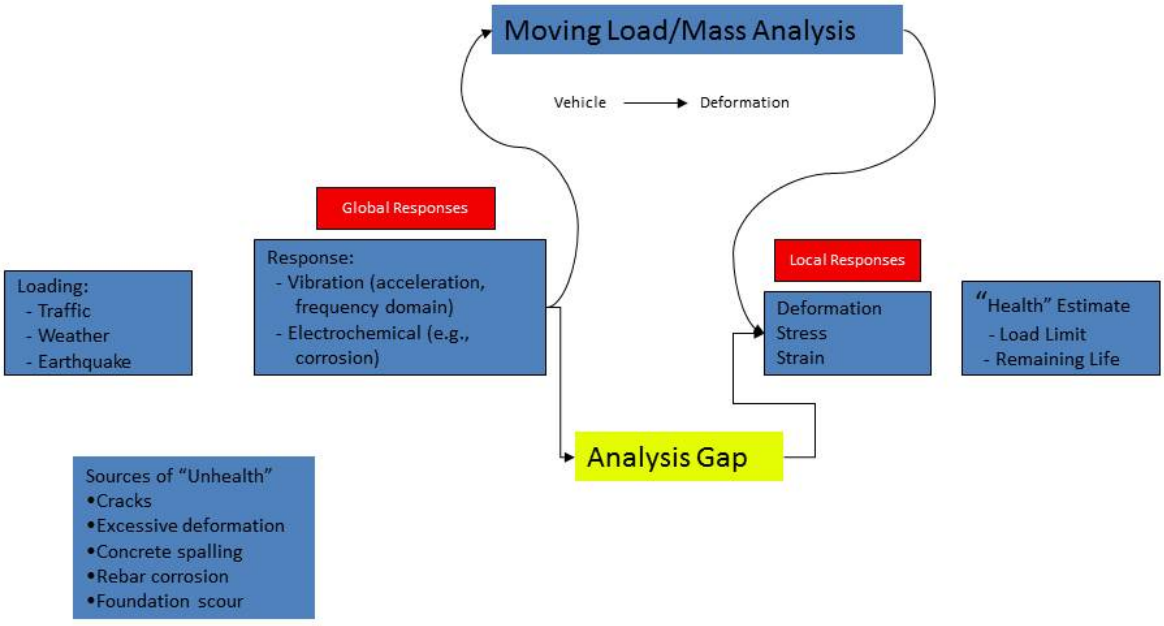

Figure 12: Proposed SHM Information Flow for Bridges

4.0 THE MOVING LOAD/MASS ANALYSIS ON BRIDGES [13]

In order to span the analysis gap (Figure 12) between large scale global parameters (such as bridge geometry, vehicle speed and weight) and local responses (such as deflection, stress, and strain), the moving mass problem is employed. The moving mass problem for one or more objects progressing over an initially stationary, flexible structure would be expressed as a series of equations of motion for the corresponding moving bodies accounting for the fact that the interaction between the objects varies spatially and temporally. Typically a constant "vehicle" velocity is assumed, and thus space and time are not independent. The equation of motion for the stationary structure is a partial differential expression with respect to location and time. For simple uniform beams there is only one spatially independent variable (parallel to the length of the beam), but for plates there are two (parallel to the length and to the width). This section explores various types of moving load and mass problems, reviews their analytical solutions (where available), and examines their solution using the ANSYS Workbench12.1 finite element software.

4.1 Simply Supported Beam with Moving Load

The moving mass problem in its simplest form is the moving load problem for a simply supported beam, as illustrated by *Frỳba* [14] and shown in Figure 13.

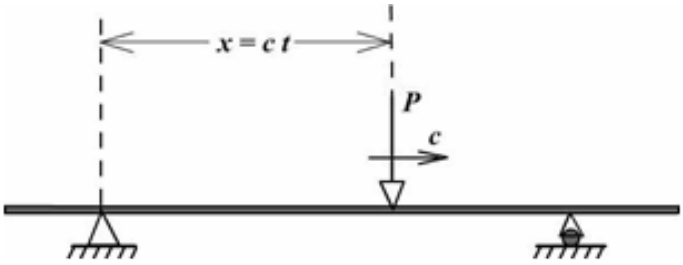

Figure 13: Beam with Moving Load [14]

In relation to a vehicle bridge interaction, the vehicle is modeled as a massless point load at a constant velocity *c*, and the bridge is represented as a uniform, simply supported Euler-Bernoulli beam. Since the force *P* is applied on a moving point, it can be represented using the Dirac Delta Function:

$$P\delta(x - ct) \tag{6}$$

where *x* is the spatial variable parallel to the length of the beam and *t* is time. The equation of motion for an Euler-Bernoulli beam is given by:

$$\mu \frac{\partial^2 w(x,t)}{\partial t^2} + 2\mu\omega_b \frac{\partial w(x,t)}{\partial t} + EI \frac{\partial^4 w(x,t)}{\partial x^4} = \sum F_i \tag{7}$$

where μ is the linear density of the beam, *w* is the vertical transverse deflection, ω_b is the circular frequency of damping, *E* is Young's Modulus, *I* is the area moment of inertia of the beam, and F_i are all input forces on the beam. Noting that the moving load is the only force on the beam, we can combine equations 6 and 7 to yield:

$$\mu \frac{\partial^2 w(x,t)}{\partial t^2} + 2\mu\omega_b \frac{\partial w(x,t)}{\partial t} + EI \frac{\partial^4 w(x,t)}{\partial x^4} = P\delta(x - ct) \tag{8}$$

Because the beam is simply supported, the deflections and moments at each support are equal to 0.

$$w(0,t) = w(L,t) = EI\frac{\partial^2 w(0,t)}{\partial x^2} = EI\frac{\partial^2 w(L,t)}{\partial x^2} = 0 \tag{9}$$

where *L* is the length of the beam. Additionally it can be assumed that the beam is initially at rest.

$$w(x,0) = \frac{\partial w(x,0)}{\partial t} = 0 \tag{10}$$

The analytical solution to this problem typically involves a Fourier transform. Using Equations 8-10 results in the analytical solution to the moving load problem for a simply supported beam [fry]:

$$w(x,t) = w_0 \sum_{n=1}^{\infty} \frac{1}{n^2[n^2(n^2-\alpha^2)^2+4\alpha^2\beta^2]}\left[n^2(n^2-\alpha^2)sin(n\omega t)\right.$$

$$-\frac{n\alpha[n^2(n^2-\alpha^2)-2\beta^2]}{(n^4-\beta^2)^{1/2}}e^{-\omega_b t}sin(\omega'_n t)$$

$$\left.-2n\alpha\beta\left(cos(n\omega t) - e^{-\omega_b t}cos(\omega'_n t)\right)\right]sin\left(\frac{n\pi x}{L}\right) \tag{11}$$

Equation 11 can be evaluated at any position and time to yield the beam deflection. To illustrate this solution using finite elements, we will create an example beam and vehicle with the following properties:

L (Beam Length) = 30.48 meters (100 feet)
b (Beam Width) = 0.6096 m (2 ft)
h (Beam Height) = 1.524 m (5 ft)
E (Modulus of Elasticity) = 200 GPa (29 Msi)
ρ (Beam Density) = 7850 $^{kg}/_{m^3}$ $\left(490\ ^{lbm}/_{ft^3}\right)$

c (Vehicle Speed) = 29 $^{m}/_{s}$ (65 mph)
P (Vehicle Weight) = 290 kN (65000 lbs)

These input properties results in the following parameters:

A (Beam Cross-Sectional Area) = 0.929 m^2 (10 ft^2)
μ (Mass Density) = ρA = 2793 $^{kg}/_{m}$ $\left(4900\ ^{lbm}/_{ft}\right)$

I (Bending Area Moment of Inertia) = $\frac{h^3 b}{12}$ = .1798 m^4 (20.83 ft^4)
ω (Applied Load Frequency) = $\frac{\pi c}{L}$ = 0.2989 $^{rad}/_{s}$
α (Speed Parameter) = $\frac{cL}{\pi}\sqrt{\frac{\mu}{EI}}$ = 0.1267
β (Damping Parameter) = $\frac{\omega_b}{\omega_1}$ = 0.01

T (Time of Traverse) = $\frac{L}{c}$ = 1.05 s

Because the analytical solution only considers the spatial dimension along the length of the beam (x) and along the thickness of the beam (w), a 2-dimensional analysis will be performed. Also, because the relationship between β and ANSYS material damping parameters is particularly convoluted, damping is left out of this model, slightly affecting its accuracy. Additionally it should be noted that although the moving load problem associates no mass with the vehicle, ANSYS is unable to form a solution matrix with massless or near massless objects. As such, for this simulation, the vehicle is given a mass comparatively small to the bridge mass: around 0.01%. Although this mass will negligibly affect the overall solution, its effect should be small. The beam and vehicle bodies shown in the Figure 14

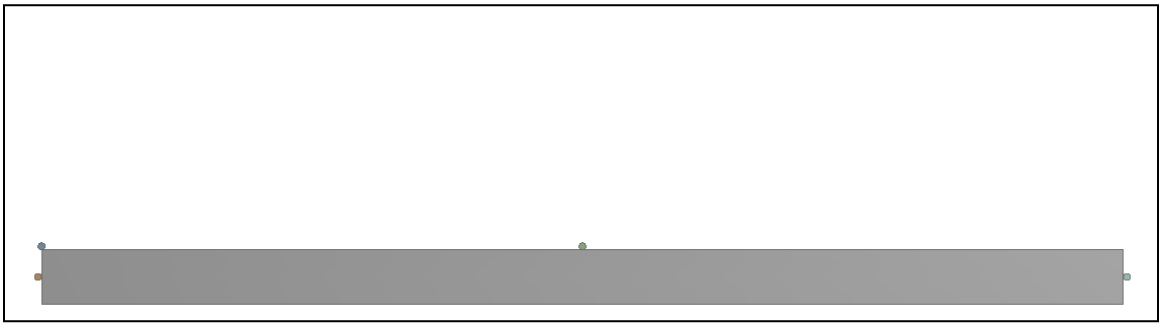

Figure 14: Simply Supported Point Load in ANSYS DesignModeler

With a solution time step in the range of 1×10^{-4} seconds and 1×10^{-2} seconds, the results are as shown in Figure 15.

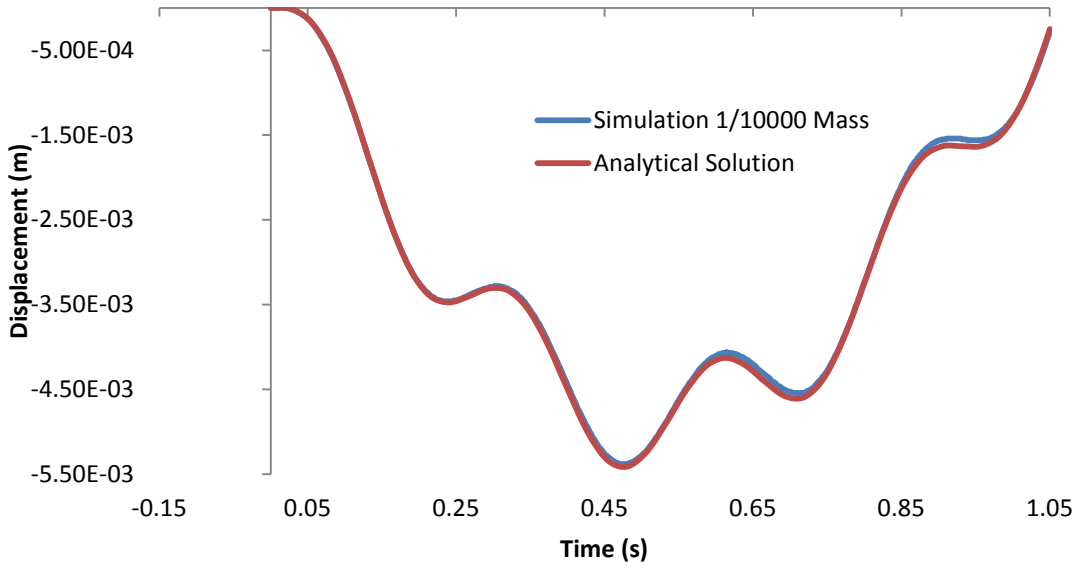

Figure 15: Simply Supported Beam Analytical Comparison

This appears plausible for the vertical motion of the center of a simply supported beam with a vehicle moving over it. When compared with the analytical solution using the first 10 modes, as shown in Figure 15, it is nearly identical. The maximum error between the objects is less than 5.5%, occurring around 0.9 seconds. This error can be attributed to the additional mass of the vehicle. As will be demonstrated next, the extra mass of the vehicle increases the inertia of the system, causing a decrease in the frequency of vibration. This effectively slows the movement of the beam, causing changes in the rate of deflection to come later in time.

4.2 Simply Supported Beam with Moving Mass

Because vehicles such as heavy transport trucks can have a significant amount of mass relative to the mass of the bridge, it would be necessary to consider this mass when formulating the problem. As such, the moving mass problem is formulated by incorporating the mass of the vehicle, moving in conjunction with the applied load; the governing equation for this problem is given in Equation 12.

$$\mu \frac{\partial^2 w(x,t)}{\partial t^2} + 2\mu\omega_b \frac{\partial w(x,t)}{\partial t} + EI \frac{\partial^4 w(x,t)}{\partial x^4} = \delta(x - ct)\left[P - m_v \frac{\partial^2 w}{\partial t^2}|_{x=ct}\right] \qquad (12)$$

where m_v is the mass of the vehicle. This is illustrated in Figure 16.

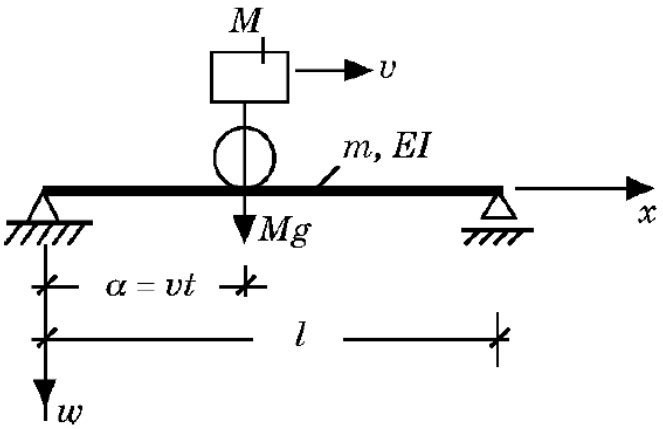

Figure 16: Beam with Moving Mass [15]

Although this PDE has no exact solution, it has been solved in many ways, including an iterative solution by Michaltsos, et al. [15]. This approach solves the equation neglecting the vehicle mass, then uses the deflection solution for the moving mass, resolving iteratively. This provides a more accurate result than other approaches, such as the one by Inglis [16] that lumps the vehicle mass at the center of the beam. Using parameters employed by Venkatesan [17] differences in prediction between the moving load and moving mass problems are as shown in Figure 17.

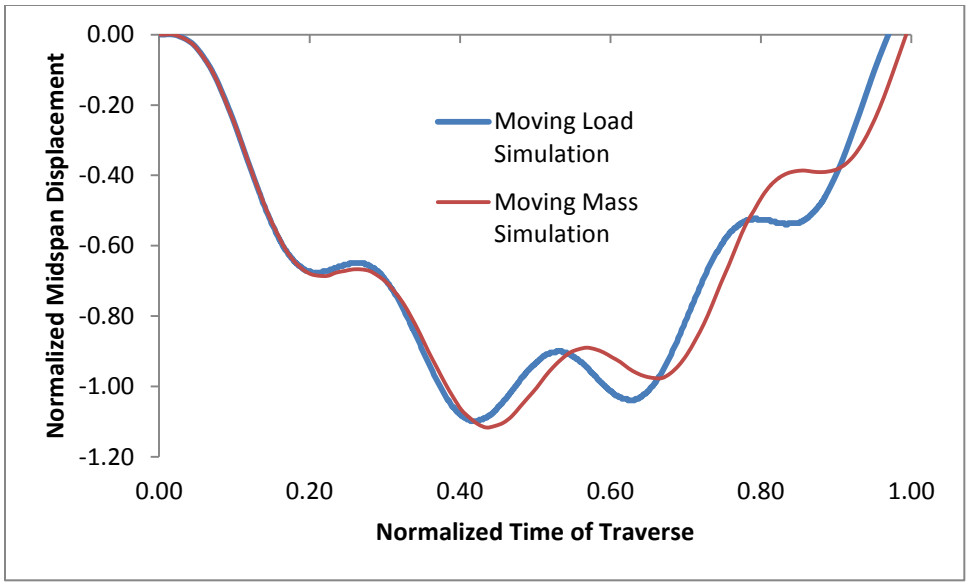

Figure 17: Moving Mass and Load Simulation Comparison

As can be seen in Figure 18 the added inertia of the vehicle mass alters the vibrating frequency of the beam found in the moving load analysis. This causes a decrease in the magnitude of the acceleration of the beam relative to the moving load system.

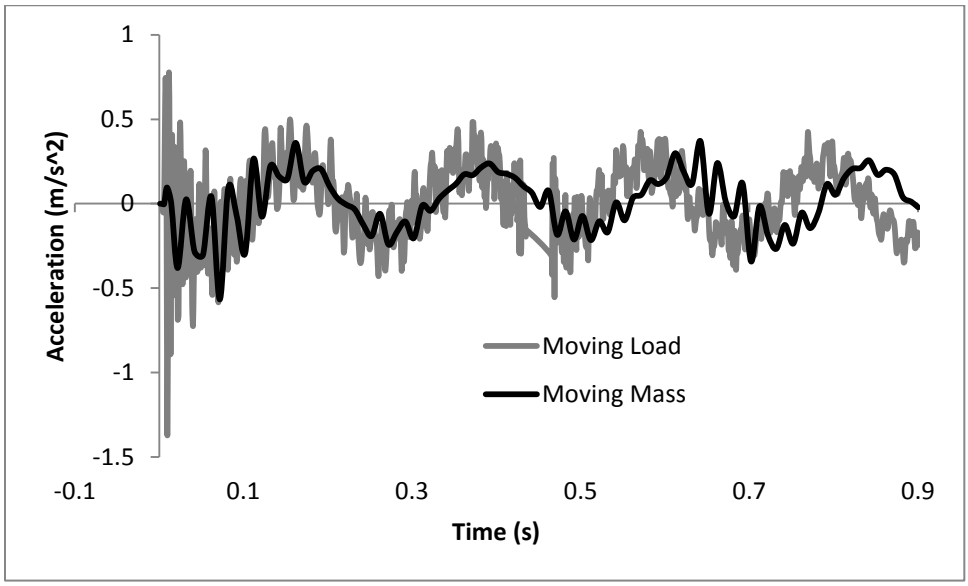

Figure 18: Moving Mass and Load Acceleration Comparison

The average magnitude of acceleration of the moving mass solution is 0.139 m/s^2, while the average magnitude of the moving load problem is 0.178 m/s^2. This is a reduction of 22.3%.

Comparison can now be made to the results obtained by Venkatesan [17] in Figure 19.

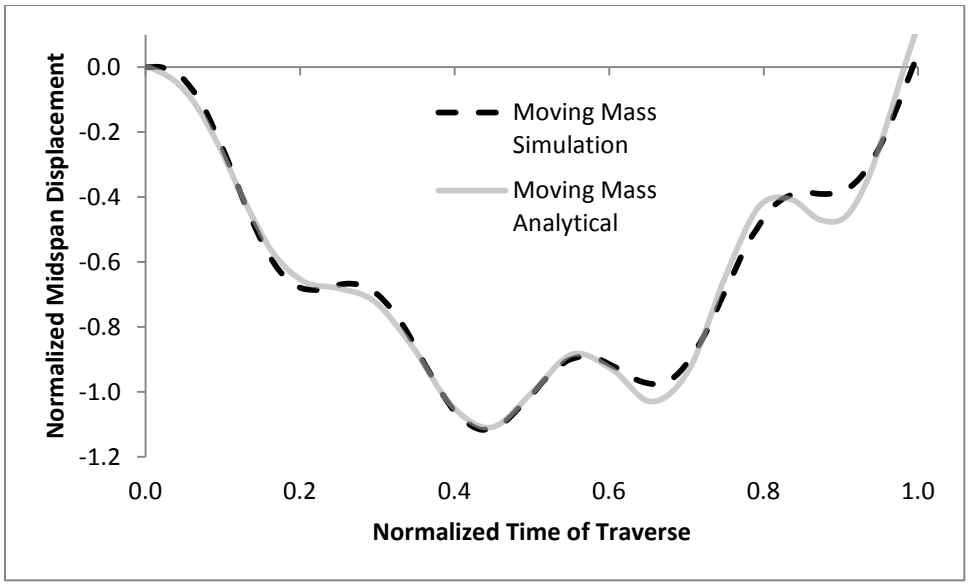

Figure 19: Moving Mass Simulation with Moving Mass Analytical Solution

Around $\tau = 0.65$ and τ = 0.85 the simulation loses accuracy amounting to about ten percent (10%) of static mid-span deflection. This can be attributed to the accumulation of small errors through iterations on an imperfect model. Fortunately, the important aspects of this analysis are to capture the maximum deformation of the bridge and the general path of its movement, which were both approximately accurately.

Other two dimensional beam-based models moving masses were solved, such as the simply support beam with a moving oscillator, the simply supported beam with multiple loads, and the simply support beam with a linked-mass, two-contact moving oscillator. Additionally, we conducted similar comparisons between analytical computational results on three-dimensional structures such as the simply supported plate with a moving load and all of the above are available in [13].

4.3 Three-Dimensional Simply Supported Beam

While the analytical solution of the previous mentioned plate problem may be relatively simple, it does not accurately represent a bridge span. Spans are only supported at the ends of the length dimension and not the width dimension. However, no work has been found that has provided an analytical solution to this type of problem without resorting to the finite element method. This section will thus create three-dimensional simulations similar to the previous two-dimensional examples for comparison. We will begin with a three-dimensional replica of the system given in Section 4.1, and then follow with the case where that mass is lumped into a central body, as is more descriptive of a vehicles motion over a bridge. This will show that two-dimensional models underestimate the deformation by ignoring the additional bending in the transverse direction.

4.3.1 Width-Distributed Moving Mass

In order to verify the use of a three-dimensional simulation, a model was constructed that was equivalent to its two-dimensional counterpart in Section 4.2. This model assures that there will be no displacement variation in the transverse direction on the beam. A solid rectangular prism body was created for the beam and simple supports were created on either end in the length direction, aligning a solid edge with the center of the height of the beam. The moving mass was

modeled as a cylinder whose primary axis is along the length of the beam. This three-dimensional beam configuration is shown in Figure 20.

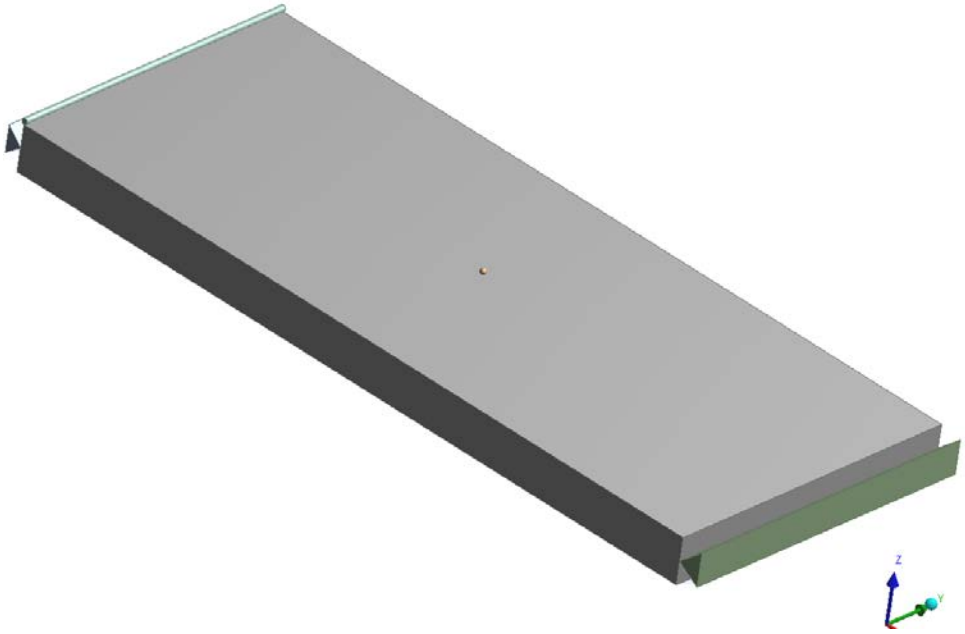

Figure 20: Isometric View of the Three-Dimensional Moving Mass Model

A force in the negative *z*-direction is placed along the face of the cylinder. The line adjoining the beam and the supports is constrained to zero displacement. All steps similar to previous analyses that are necessary for a successful run are taken. The following parameters are used for this analysis:

L (Length of Beam) = 25 m
b (Width of Beam) = 10 m
h (Height of Beam) = 1.516 m
E (Young's Modulus of Beam) = 2.87 GPa
ν (Poisson's Ratio for Beam) = 0.3
ρ (Beam Density) = 151.91 $^{kg}/_{m^3}$

P (Weight of Vehicle) = 26690 N
c (Vehicle Speed) = 27.778 $^{m}/_{s}$

Since ANSYS does not allow rotational constraints for this type of problem, the cylinder may bounce as it progresses along the beam. This was countered by reducing the stiffness of the cylinder to the proper amount to retain its form while allowing slight deformations to match the deflections of the beam; however, this was a very time consuming process. A faster solution with a relatively low amount of added error would be to model the distributed vehicle as a series of spheres instead of a cylinder. The solutions approach each other as the number of spheres increases. Each sphere could be set upon a linear path, and the minimal differences in deformation along the transverse direction of the beam will not cause loss of contact, as it would with a straight, rigid cylinder.

The results of the three-dimensional analysis are shown compared to those of the equivalent two-dimensional analysis (Section 4.2) in Figure 21.

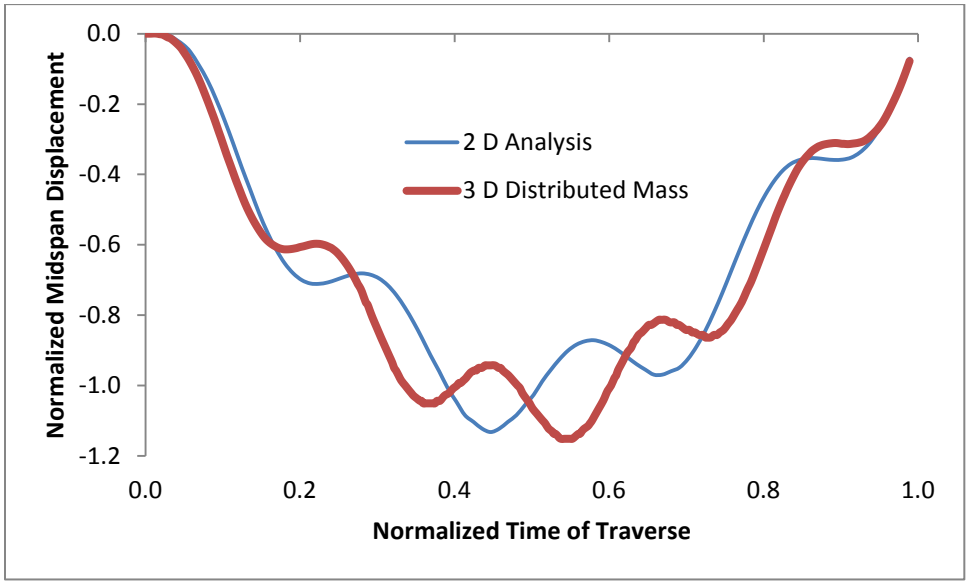

Figure 21: Verification of Three-Dimensional Analysis

The simulation has fairly accurately captured the maximum deformation and the general deflection profile; however there are some key differences between the results. These can be attributed to the nonuniformity of deflection along the transverse direction arising from the three-dimensional analysis.

4.3.2 Centrally Located Moving Mass

Unlike the model implemented in the previous problem, actual vehicles do not distribute their weight over the width of the bridge. Instead, the vehicle weight is located in what can be more closely approximated as discrete points, e.g., tire patches. As such, it is potentially advantageous to model a vehicle as a discrete point on a three-dimensional beam. Our implementation of this model is shown in Figure 22.

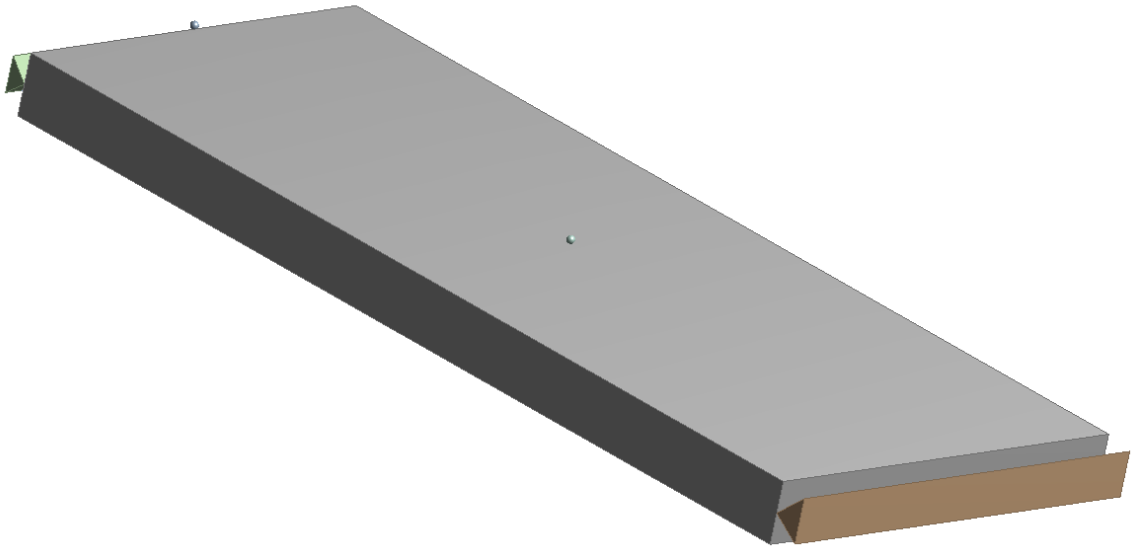

Figure 22: Three-Dimensional Lumped Moving Mass Model

The results of this analysis compared with the two-dimensional model, which allows for no response variation in the transverse direction, is given in Figure 23.

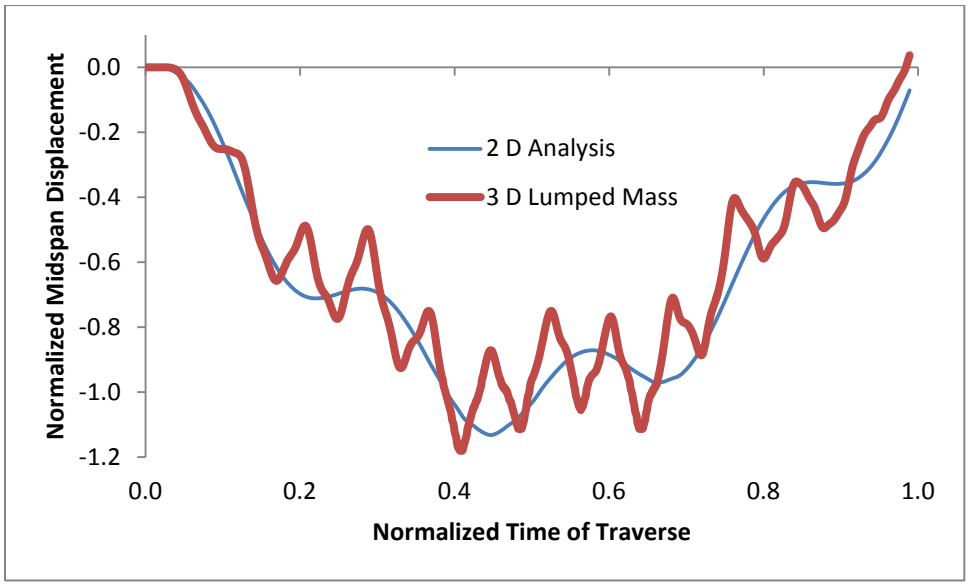

Figure 23: Comparison of Lumped and Distributed Moving Mass Models

While the overall profiles are similar, there is additional oscillation at the mid-span when the vehicle is sufficiently far from the supported ends for the lumped system. This is because the beam is free to vibrate and deflect in the transverse direction. This additional bending is best visualized by Figures 24 and 25. When considering a line in the transverse direction that stays with the vehicle body, the maximum deflection oscillates from the outside to the middle and back, as one would expect from a free-free bending vibration.

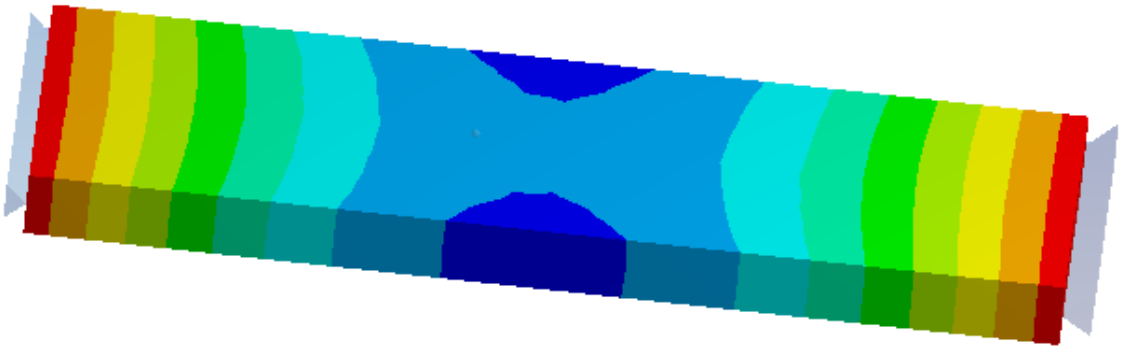

Figure 24: 3D Lumped Mass Simulation at 0.378 Seconds

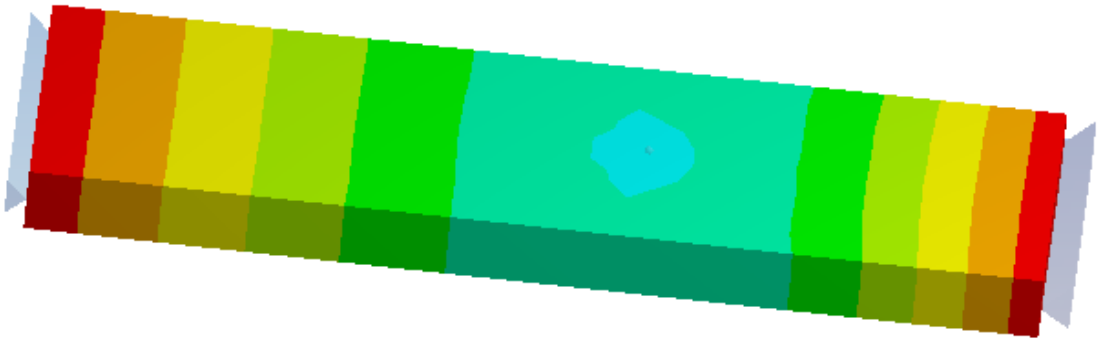

Figure 25: 3D Lumped Mass Simulation at 0.50 Seconds

As can be seen in Figure 23, the period of these oscillations is about 0.07 seconds, implying a frequency of around 14 Hz. By conducting a modal analysis on this beam, we find that the first torsional frequency of the beam is approximately 15.5 Hz; this mode shape is shown in Figure 26. Large deformations occur near the outside edges of the mid-span of the beam.

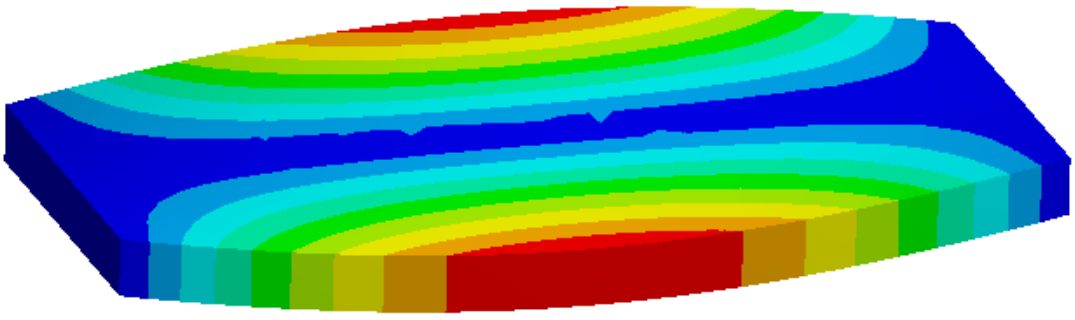

Figure 26: First Torsional Mode Shape (15.5 Hz)

This additional vibration causes a larger deflection than when only considering the length and height dimensions, as well as changes the precise deflection profile, and thus the transverse distribution of the mass of the vehicle is an important factor in the modeling of the vehicle bridge interaction.

4.4 Additional Considerations

The moving mass problem has proven to provide an accurate assessment of deflection profiles of beams when objects are traversing them. Additionally, different variations on the problem increase the accuracy by modeling certain physical qualities. Considering the mass of the vehicle is necessary as it dramatically increases the overall deflection of the beam. Distributed vehicle systems decrease the overall deflection of the beam in correlation to the relative distance between loads and the length of the beam. Also, vehicle suspension in the form of an oscillating mass can greatly affect the beam dynamics based off of the oscillating frequency related to the natural frequencies of the bridge.

Finite element simulation using ANSYS has also proven to accurately model the moving mass problem in some of its forms. Unfortunately, it is not able to consistently and accurately replicate the oscillating moving bodies for this type of simulation. As such, future models should not include oscillating bodies. Additionally, it is necessary to consider affects outside of the plane of action, particularly for beams with non-uniform cross-sections. This can greatly affect the overall deflection of the beam, and is necessary for more complicated analyses.

5.0 Conclusions

The primary products of project are the re-establishment of the data acquisition capabilities on the Walnut Creek Bridge, including off-site data transmission, a proposed new paradigm for structural health monitoring that includes a rational, quantifiable measure of structural "health", and the development of a new class of moving mass analyses for heavy vehicles on bridge structures. Operation of data acquisition system has been demonstrated and validated. The reliability-based SHM algorithm, while in its early stages of development, has been developed sufficiently to guide the associated vehicle-bridge interaction analysis via the moving mass calculations.

6.0 Implementation and Technology Transfer

Two aspects of this project will provide the most benefit to the bridge sustainment community. First, the reliability-based SHM algorithm proposed here represents the first time structural "health" has been defined clearly. To this point, researchers have claimed health monitoring without defining "health"; one cannot monitor what has not been defined. Also, as the connecting element of the analysis transferring global response data to the local level, our moving mass analyses on three-dimensional structures point the way to future analyses that should increase the fidelity of the simulations.

7.0 References

1. Patten, William N., "Semiactive Vibration Absorbers (SAVA) at the I-35 Walnut Creek Bridge", Oklahoma Department of Transportation, 1997.
2. Bhachu, Kanwardeep, *A Method to Characterize Highway Traffic for Bridge Health Monitoring*, MS Thesis, University of Oklahoma, 2009.
3. http://www.hbm.com/en/menu/products/measurement-electronics-software/rugged-data-acquisition/somat-edaqlite/, accessed 27 August 2012.
4. http://www.pcb.com/spec_sheet.asp?model=393A03&item_id=11200, accessed 27 August 2012.
5. Comments by Ray McCabe - National Director of Bridge and Tunnel Design for the Engineering and Architecture Firm HNTB, online at URL: http://www.radiospace.com/hntb.htm, and also at http://www.hntb.com/documents/pdf/HNTB_Designer88_08.pdf (Page 23).
6. http://www.nworegon.org/Assets/dept_4/PM/pdf/Reauthorization priorities paper 06-08 DRAFT.pdf, page 7, accessed 27 August 2012.
7. McCormick, Norman J., 1981, *Reliability and Risk Analysis*, Orlando, Florida: Academic Press.
8. Isaacson, Dean L., and Richard W. Madsen, 1976, *Markov Chains - Theory and Applications*, New York: John Wiley & Sons.

9. Bogdanoff, J.L., F. Kozin, and B.X. Shi, 1984, “An Approach to Non-Stationary Markov Chain Models of Cumulative Damage”, Proceedings of the Fourth ASCE Specialty Conference on Probabilistic Mechanics and Structural Reliability, pp. 380-384.
10. Harary, Frank, Benjamin Lipstein and George P.H. Styan, 1970, “A Matrix Approach to Nonstationary Chains”, Operations Research, 18(6), pp. 1168-1181.
11. Lee, T.C., and G.G. Judge, 2006, “Estimation of Transition Probabilities in a Nonstationary Finite Markov Chain”, Metroeconomica, 24(2), pp. 180-201.
12. Spirkl, Wolfgang and Harald Ries, 1986, “Non-Stationary Markov Chains for Modeling Daily Radiation Data”, Quarterly Journal of the Royal Meteorological Society, 112, pp. 1219-1229.
13. Kroll, Adam, 2011, Analysis of Finite Element Solutions to the Moving Mass Problem for Health Monitoring of the Walnut Creek Bridge
14. Fryba, L, *Vibration of Solids and Structures under Moving Loads*, Thomas Telford Ltd., Third Edition, 1999.
15. Michaltsos, G.; Sophianopoulos, D.; and Kounadis, A. N., “The Effect of a Moving Mass and Other Parameters on the Dynamic Response of a Simply Supported Beam”, *Journal of Sound and Vibration*, 1996, Volume 191(3), pgs 357-362.
16. Inglis, C. E., “A mathematical treatise on vibration in railway bridges”, The University Press, Cambridge, 1934.
17. Venkatesan, Gopinath, *Dynamic Behavior of Bridge Structures Under Moving Loads and Masses Using Differential Quadrature Method*, PhD Dissertation, University of Oklahoma, 2009.